

Polyamine-based Pt(IV) Prodrugs as Substrates for Polyamine Transporters Preferentially Accumulates in Cancer Metastases as DNA and Polyamine Metabolism Dual-Targeted Antimetastatic Agents

hanfang liu, Jing Ma, Yingguang Li, Kexin Yue, Linrong Li, Zhuoqing Xi, Xiao Zhang, Jianing Liu, Kai Feng, Qi Ma, Sitong Liu, Shudi Guo, Peng G. Wang, Chaojie Wang, and Songqiang Xie

J. Med. Chem., **Just Accepted Manuscript** • DOI: 10.1021/acs.jmedchem.9b01641 • Publication Date (Web): 25 Nov 2019

Downloaded from pubs.acs.org on November 26, 2019

Just Accepted

“Just Accepted” manuscripts have been peer-reviewed and accepted for publication. They are posted online prior to technical editing, formatting for publication and author proofing. The American Chemical Society provides “Just Accepted” as a service to the research community to expedite the dissemination of scientific material as soon as possible after acceptance. “Just Accepted” manuscripts appear in full in PDF format accompanied by an HTML abstract. “Just Accepted” manuscripts have been fully peer reviewed, but should not be considered the official version of record. They are citable by the Digital Object Identifier (DOI®). “Just Accepted” is an optional service offered to authors. Therefore, the “Just Accepted” Web site may not include all articles that will be published in the journal. After a manuscript is technically edited and formatted, it will be removed from the “Just Accepted” Web site and published as an ASAP article. Note that technical editing may introduce minor changes to the manuscript text and/or graphics which could affect content, and all legal disclaimers and ethical guidelines that apply to the journal pertain. ACS cannot be held responsible for errors or consequences arising from the use of information contained in these “Just Accepted” manuscripts.

1
2
3
4
5
6
7
8
9
10
11
12
13
14
15
16
17
18
19
20
21
22
23
24
25
26
27
28
29
30
31
32
33
34
35
36
37
38
39
40
41
42
43
44
45
46
47
48
49
50
51
52
53
54
55
56
57
58
59
60

Polyamine-based Pt(IV) Prodrugs as Substrates for Polyamine Transporters Preferentially Accumulates in Cancer Metastases as DNA and Polyamine Metabolism Dual-Targeted Antimetastatic Agents

Hanfang Liu,^{†#} Jing Ma,^{†##} Yingguang Li,[†] Kexin Yue,[†] Linyong Li,[†] Zhuoqing Xi,^{†II} Xiao Zhang,[§] Jianing Liu,^I Kai Feng,^I Qi Ma,[†] Sitong Liu,[†] Shudi Guo,[†] Peng George Wang,^{III} Chaojie Wang,^{§*} and Songqiang Xie,^{&*}

[†] School of Pharmacy, Institute for Innovative Drug Design and Evaluation, Henan University, N. Jinming Ave, 475004 Kaifeng, China

[&] School of Pharmacy, Institute of Chemical Biology, Henan University, N. Jinming Ave, 475004 Kaifeng, China.

[§] The Key Laboratory of Natural Medicine and Immuno-Engineering, Henan University, Kaifeng, 475004, China.

^I School of medicine, Henan University Minsheng College, Kaifeng, 475004, China.

^{II} Henan University of Science and Technology Second Affiliated Hospital, Luoyang, 471000, China.

^{III} The State Key Laboratory of Microbial Technology and National Glycoengineering Research Center, Shandong University, Qingdao, 266237, China.

The authors contribute equally to this work.

KEYWORDS: *Platinum drugs, Cancer, Polyamine Metabolism and Function, Anticancer and Antimetastatic Activity*

ABSTRACT: Diverse platinum drug candidates have been designed to improve inhibitory potency and overcome resistance for orthotopic tumor. However, the antimetastatic properties are rarely reported. We herein report that homospermidineplatin (**4a**), a polyamine-Pt(IV) prodrug, can potently inhibit tumor growth *in situ* and reverse cisplatin resistance as expected. And more importantly, **4a** displays remarkably elevated antimetastatic activity *in vivo* (65.7%), compared to that of cisplatin (27.0%) and oxaliplatin (19.6%). The underlying molecular mechanism indicates that in addition to targeting nuclear DNA, **4a** can modulate the polyamine metabolism and function in a different way from that of cisplatin. By up-regulating SSAT and PAO, **4a** down-regulates the concentrations of Put, Spd and Spm, which are in favor of suppressing fast-growing tumor cells. Moreover, the p53/SSAT/ β -catenin and PAO/ROS/GSH/GSH-Px pathways are involved in the **4a**-induced tumor metastasis inhibition. Our study implies a promising strategy for the design of platinum drugs to treat terminal cancer.

1. INTRODUCTION

One of the major causes of death in cancer patients and a major obstacle in present chemotherapy are tumour metastasis. Approximately 90% of cancer patient deaths are due to metastatic cancer. [1, 2] Current anticancer agents can cure well-defined primary tumour, but they have limited impacts on metastatic cells. [3-5] Pt(II) drugs and new Pt(IV) agents prevail in the treatment of cancer, but they are less effective in the treatment of metastatic tumour. [6] Thus, the design of novel antimetastatic therapeutic agents, including new Pt agents represents an area in need of urgent attention. Recently, a surge in the activity of Pt drugs, based on a great deal of mechanistic information, has been aimed at developing nonclassical Pt(IV) complexes that operate *via* mechanisms of action distinct from those of the approved drugs. [7-10] Our projects [11] and others [12] previously focused on using bioactive moieties to achieve enhanced pharmacological effects, such as the modification of axial ligands to tune lipophilicity or kinetics and the generation of dual- or multi-

targeting Pt(IV) complexes. Unfortunately, both Pt(II) and Pt(IV) complexes failed to provide simultaneous anticancer and antimetastatic activity *in vitro* and *in vivo*.

Advances in our understanding of polyamine metabolism and function and their alterations in cancer have led to resurgence in the interest of targeting polyamine metabolism as an anticancer strategy. [13a-13c] The requirements for polyamine metabolism are dysregulated in cancer, thus making polyamine function and metabolism attractive targets for therapeutic intervention. Natural products with a polyamine moiety have been found to prevent tumour cell invasion. [13d-13f] Our group [14] has provided significant evidence that some polyamine conjugates could potently inhibit tumour growth and metastasis *in vivo*. The polyamines spermidine (Spd), spermine (Spm) and their diamine precursor putrescine (Put) are naturally occurring polycationic alkylamines that are essential for eukaryotic cell growth. [13] The intracellular pathway of mammalian polyamine catabolism is a two-step process, the

Table 1. IC₅₀ (the concentration of inhibition cell proliferation by 50%) values (μM) of Pt(IV) prodrugs. Cells were treated for 48 h, and the cell viability was determined by MTT assays^[d].

	SMMC7721	Hela	MDA-MB-231	MCF-7	HCT-116	A549cisR	A549	RF ^[a]
4a	0.99±0.14	0.96±0.19	1.32±0.14	0.50±0.09	0.99±0.19	1.41±0.19	2.70±0.25	0.52
6a	15.48±1.90	10.98±1.09	ND	14.58±1.89	6.96±0.69	ND	ND	ND
8a	>20	ND	>30	>30	>20	>50	>30	ND
cisplatin	23.37±1.26	15.02±1.23	32.48±1.49	9.60±0.60	5.30±0.14	42.89±1.89	10.20±0.89	4.01
FI ^[b]	23.51	15.65	24.61	19.20	5.35	30.42	3.78	7.71
Oxaliplatin	11.77±1.88	14.17±1.29	17.72±0.89	11.62±0.78	5.89±0.29	38.97±3.23	10.00±1.23	3.90
FI ^[c]	11.89	14.76	13.42	23.24	5.95	27.64	3.70	7.50

[a] The RF (resistance factor) is defined as the IC₅₀ value in A549cisR cells/IC₅₀ value in A549 cells.

[b] FI (fold increase) is defined as IC₅₀(cisplatin)/IC₅₀(**4a**).

[c] FI (fold increase) is defined as IC₅₀(oxaliplatin)/IC₅₀(**4a**).

[d] An average of three measurements. ND = not determined.

rate of which is controlled by the activity of the inducible enzymes spermidine/spermine N1-acetyltransferase (SSAT) and N1-acetyl polyamine oxidase (PAO). Moreover, polyamine transporters (PTs) are also overexpressed in most types of cancer cells, the identity of which is still unknown. [13-14] Therefore, polyamine conjugates have become an appealing strategy for the targeted delivery of anticancer drugs with antimetastatic activity.

Moreover, recent advances in p53 regulation of ammonia metabolism through the urea cycle controlling polyamine biosynthesis and catabolism indicate that polyamine metabolism and function are closely associated with cisplatin resistance. [15] Targeting polyamine metabolism and function may imply a practical strategy for the design of Pt drugs to overcome cisplatin resistance in a totally new field.

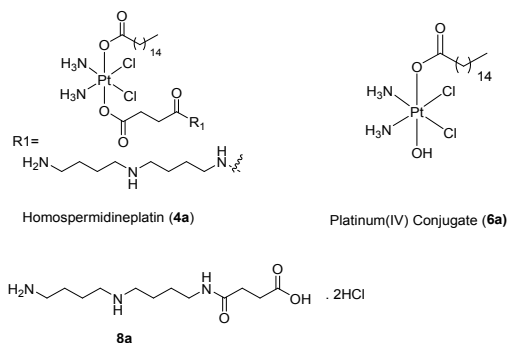


Figure 1. Chemical structures of homospermidineplatin (**4a**), Pt(IV) prodrugs without polyamine modified **6a** and the released polyamine-ligand **8a**.

Based on the key role of polyamine in mediating antitumor and antimetastatic efficacy, we rationally designed multi-action Pt prodrugs targeting polyamine function and metabolism. We firstly designed and synthesized polyamine-Pt(IV) conjugates **4-5** with the classical unsymmetrically-substituted polyamine analogs **1-3**, some of which have entered Phase III clinical trials. [13a-13c] (Figure 1 and Figure S1) Two clinical Pt(II) drugs, cisplatin and oxaliplatin, were

selected for the construction of Pt(IV) complexes **4-7** to investigate the influence of different Pt cores on antitumor activity. Compounds **6a** and **7a**, without a polyamine modification, were also designed to investigate the targeting properties of polyamine. We also synthesized the released polyamine-ligand **8a** to study how the effects come about. Feasible routes to **4-8** were established in Scheme S1-S3.

2. RESULTS AND DISCUSSION.

2.1 Synthesis and characterization of polyamine-Pt(IV) conjugates.

We established feasible routes to **4-5** (Scheme S1-S3) given in detail in the supporting information. The asymmetrically functionalized Pt(IV) compounds **e** and **z** can be obtained by the reaction of oxide-cisplatin and oxide-oxaliplatin with palmitic anhydride and then succinic anhydride. [12a] In this series, compounds **4-5** bear a hydrophobic polyamine chain varying in connecting formats from **d** (4+4), **q** (3+3+3) to **y** (3+3+3). The solid was filtered, washed several times with absolute ethanol, and dried under vacuum to give the pure target compound **4-5**. All new compounds were characterized by ¹H, ¹³C, ¹⁹⁵Pt NMR spectroscopy, ESI-MS (Figures S2-S29) and CHN elemental analysis.

2.2 The stability of **4a**.

The stability in water was evaluated using compound homospermidineplatin (**4a**). We observed that **4a** is highly stable in water, as evidenced by no change in the HPLC chromatogram after 24 h. (Figure S30) [12] And approximately 70% of **4a** remained unchanged even after 48 h in RPMI 1640, suggesting that the compound is stable in biological media. Pt levels in A549 and A549cisR cells with no dependence on aminoguanidine (AG) indicated improved metabolic stability. (Figure S31) [13f]

2.3 *In vitro* cytotoxicity effects.

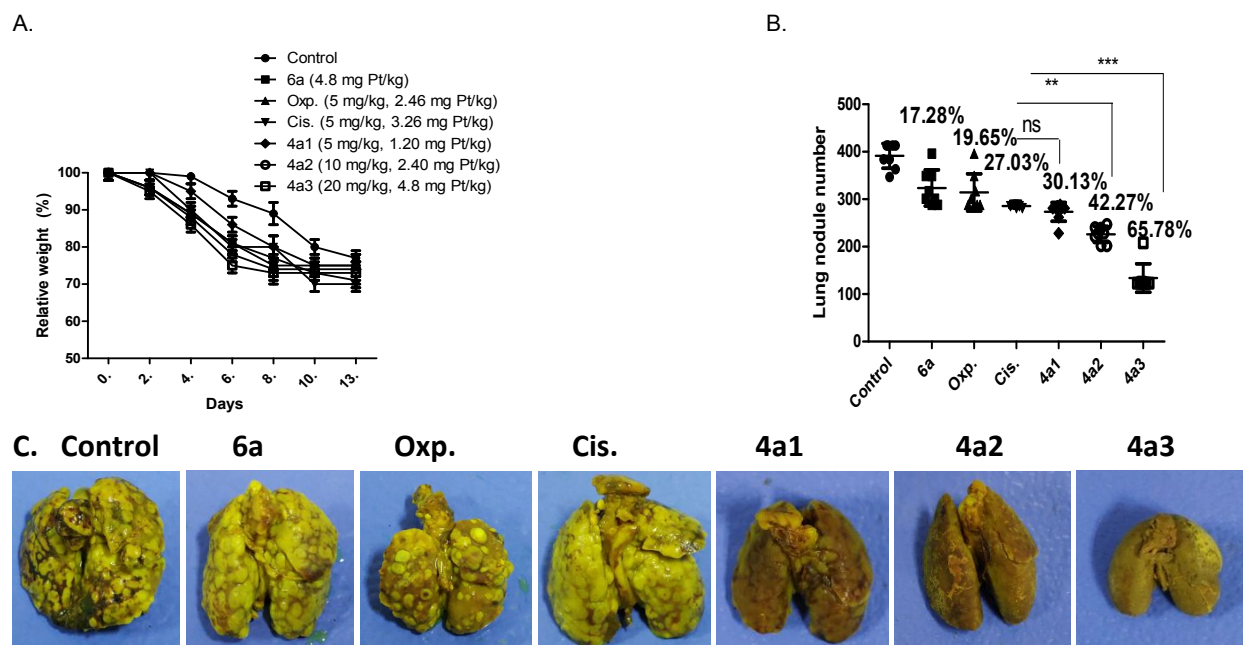


Figure 2. *In vivo* antimetastatic activity of **4a**, **6a**, cisplatin and oxaliplatin in 4T1 breast carcinoma tumors every two days for a total of four treatments. A) Body weight of mice during treatment with **4a**, **6a**, cisplatin, oxaliplatin, and control group for 14 days. B) Statistics of lung metastasis nodules from mice after treatment with **4a**, **6a**, cisplatin, oxaliplatin, and control group for 14 days. C) Representative images of pulmonary metastasis from mice treated with control, **6a** (14 mg/kg, 4.8 mg Pt/kg), oxaliplatin (5 mg/kg, 2.46 mg Pt/kg), cisplatin (5 mg/kg, 3.26 mg Pt/kg), **4a1** (5 mg/kg, 1.20 mg Pt/kg), **4a2** (10 mg/kg, 2.40 mg Pt/kg), **4a3** (20 mg/kg, 4.80 mg Pt/kg) by intravenous delivery once every two days (n = 8 mice per group). **P < 0.01; ***P < 0.001.

The *in vitro* anticancer activity of these newly synthesized polyamine-Pt(IV) compounds was assessed by using the MTT assay (Table 1 and Table S3). [15c-15d] The oxaliplatin-based Pt(IV) compound **5a** is less active than the corresponding cisplatin-based analog **4c**. For cisplatin-based scaffolds (**4a-4c**), **4a** with the homospermidine moiety is more potent than its alkynyl (**4b**) and cyclopropyl (**4c**) counterparts. **4a** is significantly more active than cisplatin and oxaliplatin in all of the tested cancer cells with some potencies in the nanomolar range, IC₅₀ values of which is almost 30 folds lower than cisplatin and oxaliplatin. The RF (resistance factor) values of polyamine-platinum(IV) conjugates **4** and **5** (RF 0.24-0.84) are 5-17 folds lower than that of cisplatin (RF=4.01), indicating its better ability to overcome cisplatin resistance. Moreover, polyamine-platinum(IV) conjugates **4** and **5** (SI 1.47-4.52) show lower cytotoxicity in normal cells HL-7702, with selectivity index (SI) values 3-12 folds higher than those of cisplatin and oxaliplatin. (Table S4) A similar tendency was observed by ICP-MS (Figure S32).

Additionally, polyamine-platinum(IV) conjugate **4a** exhibited better cell-killing effects than the Pt(IV) prodrugs **6a**, **7a** without polyamine modified, and especially the released polyamine-ligand **8a** (Table 1), indicating that polyamine plays an important role in the synthesized platinum(IV) conjugates. Among these compounds, **4a** displays the highest cytotoxicity. Therefore, we focus on **4a** for the following tests.

2.4 *In vivo* antitumor and antimetastatic activities.

Our group [14] and others [13] emphasize the importance of the potential antimetastatic activities of polyamine conjugates. And cisplatin is well known to be a poor metastasis inhibitor.

To evaluate if **4a** with a polyamine motif can prevent the tumor metastasis, the *in vitro* transwell assay was conducted. Compared with cisplatin, **4a** could inhibit breast cancer migration more potently in a dose-dependent manner as illustrated in Figure S33. This prompted us to further test the *in vivo* antitumor and antimetastatic activities of **4a**.

As shown in Table S3, the IC₅₀ of **4a** in MCF-7 cells is 0.50 μM, which is the highest in all tested cancer cells, indicating a better therapeutic effect in breast cancer. Cellular drug uptake and DNA platination of **4a** in the lung carcinoma cell lines A549 and A549cisR, the hepatocellular carcinoma cell line SMMC-7721 and the breast cancer cell line MCF-7 were also tested by ICP-MS (Figure S34). The highest Pt levels in MCF-7 suggest a potential therapy for breast cancer. Therefore, we tested the *in vivo* antitumor and antimetastatic activities of **4a** in the breast cancer model.

Metastasis is the main factor affecting mortality in cancer patients, and the lung is one of the most common sites. [16] Therefore, we injected 4T1 breast cancer cells *via* the tail vein to assess whether **4a** was effective against pulmonary metastasis *in vivo*. Surprisingly, **4a** significantly reduced the number of tumour metastatic nodules (65.78%) as shown in Figure 2, which was 3-fold higher than that of cisplatin (27.03%) and oxaliplatin (19.65%). In addition, the body weight of the mice after treatment with **4a** showed no significant difference with the control group (Figure 2A). Moreover, the variations in the organ weight indices implied that **4a** had no obvious patholog-

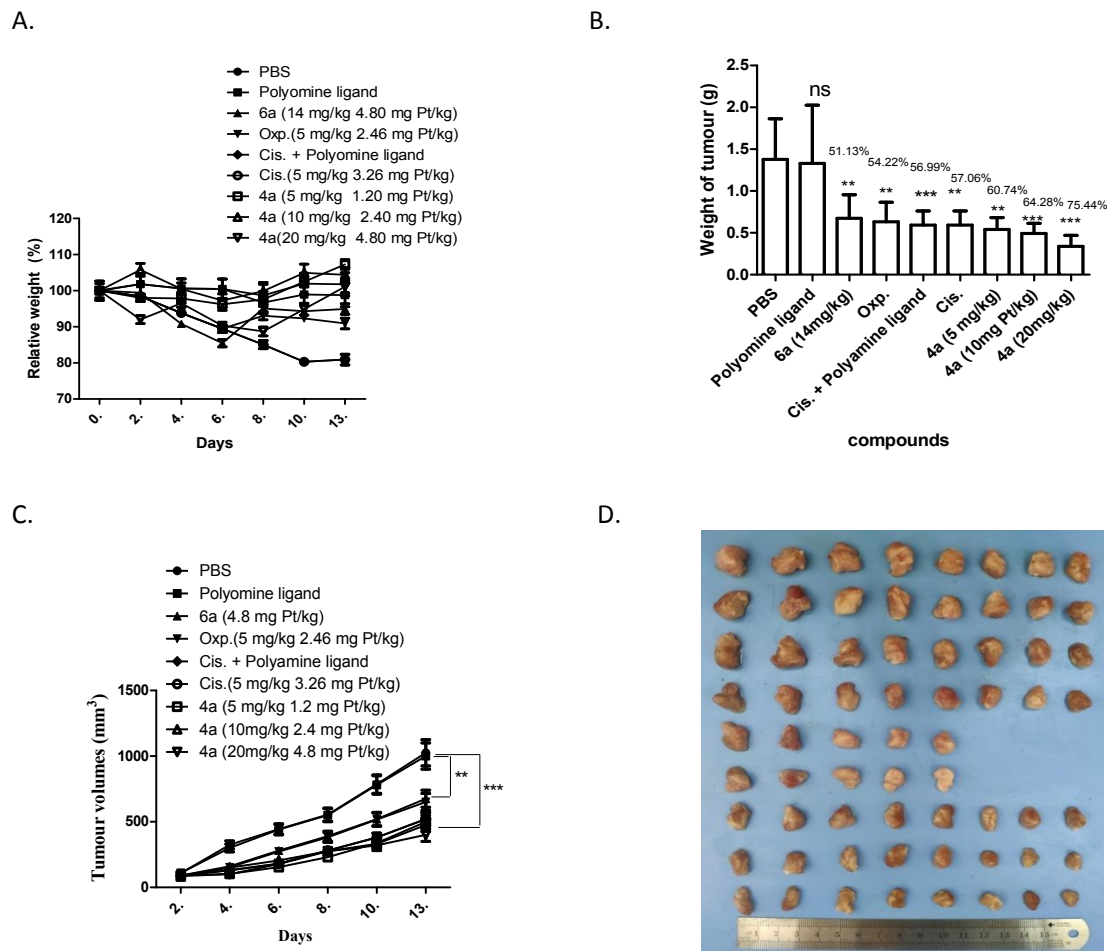


Figure 3. *In vivo* antitumor activity of **4a**, polyamine ligand **8a**, **6a** without polyamine modified, cisplatin and oxaliplatin in 4T1 breast carcinoma tumors. Eight mice each received the vehicle, cisplatin (5 mg/kg, 3.26 mg Pt/kg), oxaliplatin (5 mg/kg, 2.46 mg Pt/kg), cisplatin + Polyamine ligand (1:1, 5 mg/kg cisplatin + 5 mg/kg Polyamine ligand), **4a** (5 mg/kg, 1.20 mg Pt/kg; 10 mg/kg, 2.40 mg Pt/kg; 20 mg/kg, 4.80 mg Pt/kg) **6a** (14 mg/kg, 4.8 mg Pt/kg) or **8a** (20 mg/kg) intravenously (i.v.) every two days for a total of four treatments. A) Body weight of the mice during treatment. B) Tumor weight in each group at the end of the experiment. C) Tumor growth as a function of time. D) Images of the tumors at the end of the experiment. First horizontal line, control group; Second line, polyamine ligand **8a** group; Third line, **6a** group; Fourth line, oxaliplatin group (5 mg/kg, 2.46 mg Pt/kg); Fifth line, cisplatin + Polyamine ligand group; Sixth line, cisplatin group (5 mg/kg, 3.26 mg Pt/kg); Seventh line, **4a** group (5 mg/kg, 1.20 mg Pt/kg); Eighth line, **4a** group (10 mg/kg, 2.40 mg Pt/kg); Ninth line, **4a** group (20 mg/kg, 4.80 mg Pt/kg). **, $P < 0.01$; ***, $P < 0.001$.

ical changes compared with the control group in the *in vivo* toxicological profile experiments (Figure S35).

To further evaluate the potential safety of the polyamine conjugates *in vivo*, we conducted an acute toxicity study of **4a**, **6a**, cisplatin and oxaliplatin using BALB/c mice aged 5 weeks. Both the MTD and LD₅₀ values of **4a** are nearly 6-10 folds higher than those of **6a**, cisplatin and oxaliplatin in Table S5. The ratios of the cytotoxicity (IC₅₀) to MCF-7 cells to the animal lethal dose values (LD₅₀) of **4a** were used as a measure of the therapeutic index. [12a] The results show that **4a** is the safest complex with a therapeutic index over 33-fold higher than that of the clinical drug cisplatin and oxaliplatin.

We also tested the *in vivo* antitumor activity of **4a** in the breast cancer model. (Figure 3) On day 13, the average tumour volume was 1025 mm³ for the control group and 400 mm³ for **4a**, which was 61% and 36% lower than that of the control and oxaliplatin-treated groups, indicating marked antitumor

activity *in vivo*. Upon **4a** treatment, the tumour weight decreased significantly to 29% of that in the control group. **4a**, with the inhibition ratio of 75.44%, was better than that of cisplatin (57.06%) and oxaliplatin (54.22%). Furthermore, the acceptable toxicity of **4a** was confirmed by measuring the change in body weight (Figure 3A). After the last injection, the body weight of **4a** returned to 107% and cisplatin down to 80% of the initial weight. These results indicate that **4a** is highly efficient in inhibiting tumour growth *in vivo*. Moreover, the variations in the organ weight indices of **4a** had no obvious pathological changes compared with the control group in the *in vivo* toxicological profile experiments (Figure S36).

2.5 **4a** is transported by PTs.

For the first time, we found the rational discovery and evaluation of homospermidineplatin (**4a**), a polyamine-Pt(IV)

prodrug providing simultaneous enhanced anticancer and antimetastatic activity *in vitro* and *in vivo*. More efforts were thus conducted to illustrate the underlying molecular mechanism.

One crucial question in polyamine-conjugate chemistry is whether **4a** is actively transported by PTs. [13, 14] Spd, a natural PTs ligand, is usually used to compete with the polyamine conjugate for the PTs. The reduced cellular concentration of the polyamine conjugate by the added Spd indicated that the polyamine conjugate enters the cell by PTs. Cellular uptake and platination of nuclear DNA were first monitored in the absence and presence of Spd (Figure S37). A 68% reduction in cellular uptake and a 50% reduction in nuclear DNA were observed in the presence of 20 μ M Spd. Under similar conditions, the cellular uptake of **6a** and cisplatin did not significantly change. The same results can be observed in MCF-7 cells in Figure S38. It is reasonable that an increase in the cellular viability (23%) of **4a** with Spd, accompanied by the reduced drug accumulation was also observed in Figure S37C. In summary, the uptake assays support the hypothesis that PTs were at least partially involved in the cellular entrance of **4a**.

2.6 The cellular accumulation and distribution of Pt in A549 and A549cisR cells.

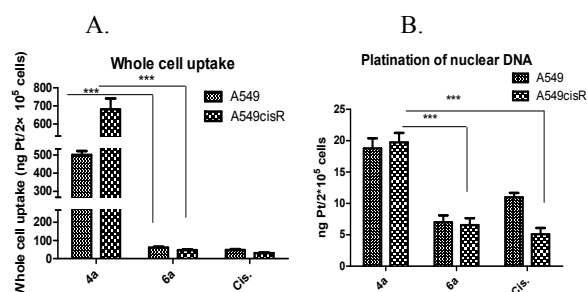


Figure 4. Cellular uptake and distribution following 8 h incubation with 10 μ M **4a** in A549 and A549cisR cells. A) Pt accumulation in A549 and A549cisR cells upon 10 μ M treatment for 8 h. B) Platination levels of nuclear DNA extracts from A549 and A549cisR cells after 8 h incubation with 10 μ M tested compounds. ***, $P < 0.001$.

Next, the cellular accumulation and distribution of Pt in A549 and A549cisR cells were measured (Figure 4). The Pt accumulation of **4a** in A549cisR cells was almost 23 times greater than cisplatin and **6a**. (Figure 4A) And also the Pt levels in A549cisR and A549 genomic DNA were 19.74 and 18.78 ng Pt per 2×10^5 cells, respectively, which was 2-6 folds higher than cisplatin and **6a**. (Figure 4B)

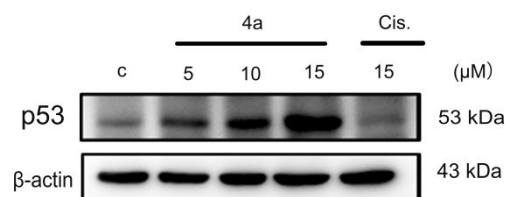
2.7 Apoptosis induced by DNA damage and DNA binding properties after reduction.

To further determine if apoptosis was induced by DNA damage, flow cytometry experiments using Annexin V/PI double staining were conducted. (Figure S39) Treatment with **4a** (5 μ M) resulted in A549cisR cell apoptosis with early apoptotic cells (33.00%) and late apoptotic cells (37.50%), which was higher than that of cisplatin (15 μ M). We also investigated the reduction and DNA binding properties of cisplatin and **4a** with ascorbic acid using 5'-dGMP as the DNA model for the inherent proficiency of the Pt prodrugs to

bind at the N7 position of guanine bases. [11] The fractions that contained unknown peaks were separated and identified by ESI-MS analysis, observing the same products as cisplatin. (Figure S40 and Table S6) The higher FI of inhibition ratio for **4a**/cisplatin with the same Pt levels in genomic DNA in A549cisR cells (Figure S41) indicated that the mechanism of **4a** was different from that of cisplatin. (Table S7)

We further examined the expression levels of phospho-histone H2A-X (Ser139) by immunoblotting (Figure S42) to determine whether **4a** is able to cause DNA damage. [17] We can see a slight increase of phospho-histone H2A-X (Ser139) after treatment with **4a** compared with cisplatin and **6a**.

A.



B.

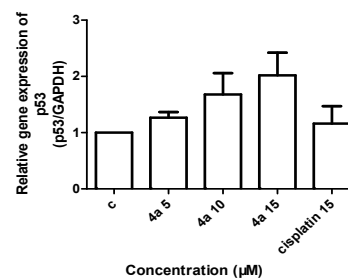


Figure 5. Effects of different concentrations of **4a** and cisplatin on p53 protein and gene expression in A549cisR cells. A) Effect of **4a** and cisplatin on p53 protein in A549cisR cells after 24 h treatment. B) qRT-PCR analysis of the p53 transcriptional level was performed with total RNAs purified from A549cisR cells treated with **4a** and cisplatin after 24h.

Due to the weak influence of **4a** on phospho-histone H2A-X (Ser139), we tested the change of p53 gene and p53 protein, which also plays an important role in cell apoptosis and cisplatin resistance. We observed after treatment with **4a**, the p53 protein and p53 gene were 3 folds higher levels than cisplatin (Figure 5). Recently, it is reported ureagenesis and ammonia metabolism including SSAT have a great influence on p53. [15] Markedly higher levels of the polyamines including Put, Spd, and Spm (Figure 5B) and a lack of p53 function (Figure 4) in A549cisR cells treated by cisplatin were observed for the first time, which was totally in contrary to **4a**, indicating that polyamine metabolism and function are good targets to overcome cisplatin resistance and targeting polyamine metabolism and function is a practical strategy for the design of Pt drugs to overcome cisplatin resistance in a totally new field. We next examined polyamine metabolism and function because such properties maybe the main factors significantly affecting the activity of **4a**.

2.8. By promoting p53/SSAT/ β -catenin and PAO/ROS/GSH/GSH-Px pathway, **4a** significantly inhibits tumour metastasis and overcomes cisplatin resistance.

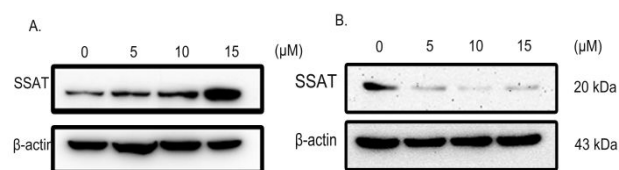


Figure 6. Effects of different concentrations of **4a** (A) and cisplatin (B) on SSAT expression in A549cisR cells after 24 h treatment.

Next, two key catabolism enzymes SSAT and PAO in polyamine cycle were determined to explore the detailed reason. We found **4a** markedly up-regulated the expression of SSAT in A549cisR cells (Figure 6A), which is totally opposite to cisplatin (Figure 6B). Our group also found that the β -catenin signalling pathway is vital in SSAT-regulated cell migration and invasion [14]. Next, β -catenin was also determined. The down-regulation of β -catenin after treatment with **4a** indicates significant antitumor migration activity, which also cannot be observed in cisplatin group (Figure 7).

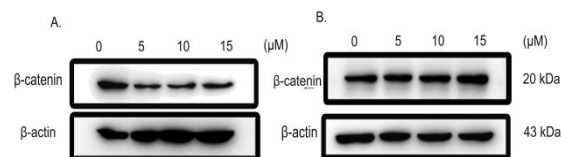


Figure 7. Effect of **4a** (A) and cisplatin (B) on β -catenin expression in A549cisR cells with 10 μ M after 24 h treatment.

In addition to SSAT, PAO is another critical catabolism enzyme. Moreover, one of the crucial reasons for Pt drug resistance is that Pt drugs are easily poisoned by S-containing proteins. [6, 7a] Cisplatin bound to a S-containing protein is immediately excreted through multidrug resistance protein. [6, 7a, 18] By raising the levels of PAO, polyamine conjugates can also up-regulate oxidizing substances ROS and down-regulate reducing substances such as GSH and GSH-Px to overcome cisplatin resistance. Surprisingly, we found that the relative PAO activity upon **4a** treatment is almost 2-10 folds higher than **6a**, **8a** and cisplatin (Figure 8A and 8B). Our group previously reported [19] a significant accumulation of ROS is closely related to PAO activity.

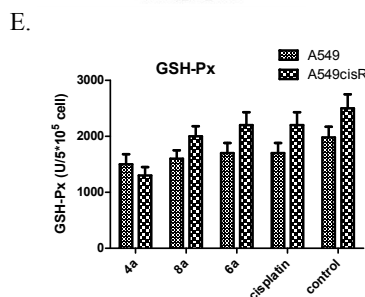
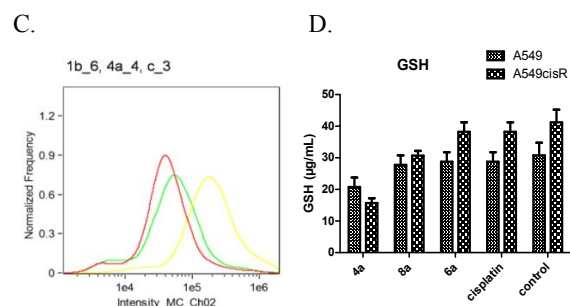
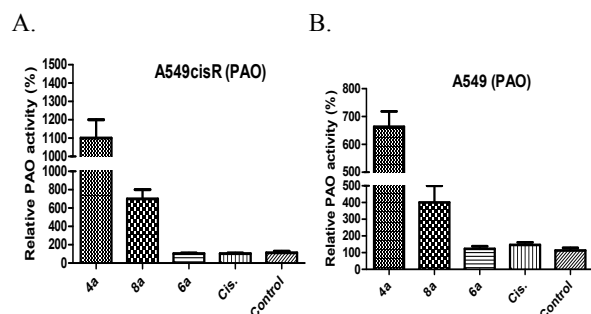


Figure 8. **4a** affects polyamine metabolism and function by upregulating PAO and ROS and downregulating GSH and GSH-Px. (A) Effect of **4a**, **8a**, cisplatin and **6a** on PAO expression in A549cisR cells with 10 μ M after 24 h treatment. (B) Effect of **4a**, cisplatin and **6a** on PAO expression in A549 cells with 10 μ M after 24 h treatment. (C). Effect of **4a**, cisplatin and **6a** on ROS expression in A549cisR cells with 10 μ M after 24 h treatment. (Yellow, homospermidineplatin **4a**; Green, cisplatin; Red, control group) (D, E) GSH and GSH-Px expression in A549 and A549cisR cells after 24 h treatment by **4a**, **8a**, **6a** and cisplatin, respectively.

The ROS content measured by FCM (flow cytometry) (Figure 8C) in A549cisR cells after treatment with **4a** was also higher than that of cisplatin. High levels of oxidizing ROS can decrease reducing substances, such as GSH and GSH-Px. GSH and GSH-Px content in A549cisR cells upon 10 μ M **4a** treatment were 3-fold lower than the control group in Figure 8D and 8E. The significantly elevated cellular levels of PAO are believed to be among the major reasons for the marked cytotoxicity of **4a** to overcome cisplatin resistance. We also found the P-gp is also partially involved in the mechanism of **4a** to overcome cisplatin resistance. (Figure S43)

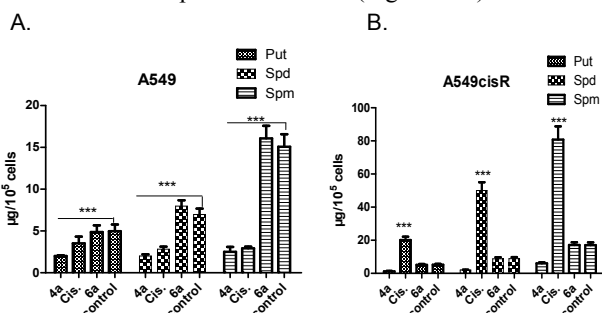


Figure 9. Effect of **4a**, **6a**, and cisplatin on polyamine metabolism and function. Polyamine (Put, Spd, and Spm) concentrations in A549 (A) and A549cisR cells (B) after 24 h treatment with or without **4a** were determined. Cisplatin and **6a** are the reference drugs. *** $P < 0.001$.

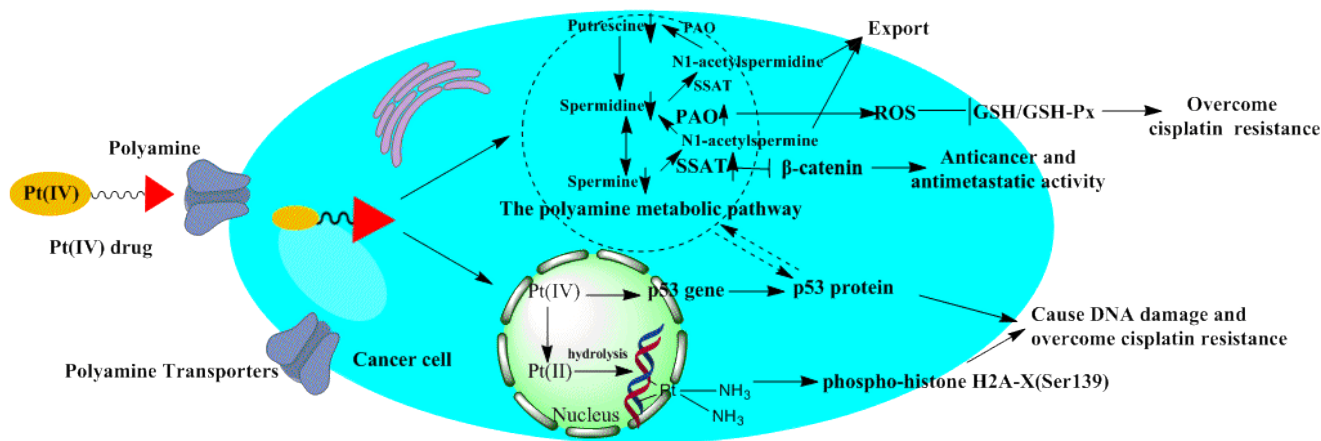


Figure 10. Proposed mechanism of action for polyamine-Pt(IV) prodrugs.

4a significantly upregulated two key catabolism enzymes SSAT and PAO in polyamine cycle. The upregulated SSAT and PAO can decrease the concentrations of Put, Spd and Spm to promote polyamine metabolism and suppress fast-growing tumour cells. Next, the contents of endogenous polyamine, Spm, Spd, and Put in A549 and A549cisR cells were measured, which plays an important role in polyamine metabolism and function (Figure 9). [13] Compared with **6a**, cisplatin and the control group, **4a** preferentially down-regulated the concentrations of Put, Spd and Spm in A549 and A549cisR cells. Moreover, the significant down-regulated SSAT and p53, and up-regulated Put, Spd and Spm (Figure 9B) after treated with cisplatin in A549cisR cells, which is totally opposite to **4a**, imply that targeting polyamine metabolism and function is a practical strategy for the design of Pt drugs to overcome cisplatin resistance in a totally new field.

3. CONCLUSIONS

Taken together, our findings provide the first example of polyamine-platinum(IV) prodrugs, targeting polyamine catabolic enzyme SSAT and PAO by PTs to regulate tumour high polyamine microenvironment and overcome cisplatin resistance, providing simultaneous enhanced anticancer and antimetastatic activity. (Figure 10) Prodrug **4a** induces apoptosis and causes DNA damage by up-regulating the p53 gene and p53 protein. The possible mechanism of polyamine-Pt(IV) complexes is targeting SSAT and PAO to down-regulate Put, Spd and Spm in A549cisR cells, which is totally opposite to cisplatin. The β -catenin signalling pathway is vital in **4a** regulated cell migration and invasion *in vitro* and *in vivo*. By raising the levels of PAO, polyamine conjugates up-regulate oxidizing substances ROS and down-regulate reducing substances such as GSH and GSH-Px to overcome cisplatin resistance.

The discovery of the potential role of homospermidineplatin, a polyamine-Pt(IV) prodrug, broadens our strategy for the design of more potential antimetastatic agents, although the details of the homospermidineplatin antimetastatic mechanism require further exploration. Markedly higher levels of the polyamines Put, Spd, and Spm, the down-regulation of SSAT and a lack of p53 function after treatment with cisplatin in

A549cisR cells imply that polyamine metabolism and function are good targets to overcome cisplatin resistance, which is totally opposite to polyamine-Pt(IV) prodrug. This evidence may be beneficial to the discovery of new Pt drugs to overcome cisplatin resistance in a totally new field and the treatment of terminal cancer.

4. EXPERIMENTAL

4.1 HPLC Studies.

The purities of all target compounds were determined by HPLC (Waters E2695-2998 equipped with a Venusil MP C18 column (150 × 4.6 mm, 5 μ m). The purity of the platinum complexes (4 - 7) were confirmed to be $\geq 95\%$ by analytical HPLC. Method for determining the purity of target compounds and the purities results were shown in Table S1 and S2, respectively.

4.2 General Procedure for the Synthesis of Compound **4a1**.

To a solution of **e** (0.38 mmol) in DMF (10 mL) was added a DMF solution (0.5 mL) containing HATU (0.57 mmol). This mixture stirred for 10 min at room temperature. A DMF solution containing **d** (1.5 mmol) and DIPEA (0.92 mmol) was added to the resulting solution. The mixture was stirred at room temperature for 24 h in the dark. The DMF was then removed under vacuum to afford a yellow oil. Compound **4a1** was purified by silica gel column chromatography as a yellow solid in a yield of 50%. $^1\text{H NMR}$ (300 MHz, MeOD) δ = 3.17 - 3.10 (m, 2H), 3.11 - 2.78 (m, 6H), 2.71 - 2.53 (m, 2H), 2.46 (s, 2H), 2.38 - 2.20 (m, 2H), 1.55 (t, $J=16.9$, 8H), 1.43 (d, $J=7.2$, 28H), 1.27 (s, 16H), 0.91 (t, $J=16.6$, 3H). $^{13}\text{C NMR}$ (300 MHz, MeOD) δ = 175.08, 174.30, 164.74, 158.27, 157.17, 80.47, 80.10, 55.67, 40.87, 40.39, 40.08, 37.00, 32.95, 30.71, 30.37, 28.77, 28.18, 27.51, 26.90, 23.63, 14.51.

4.3 General Procedure for the Synthesis of Compound **4a**.

Intermediate **4a1** was dissolved in EtOH (10 mL) and stirred at 0 $^\circ\text{C}$ for 10 min. Then, 4 M HCl was added dropwise

at 0 °C. The reaction mixture stirred at room temperature for 24–48 h and monitored by TLC. The solution typically gave a faint yellow solid as a precipitate. The solid was filtered, washed several times with absolute ethanol, and dried under vacuum to give the pure target compound **4a**. ¹H NMR (300 MHz, MeOD) δ = 3.19 (d, *J*=20.4, 6H), 2.95 (dd, *J*=17.3, 7.4, 6H), 2.53 (t, *J*=6.2, 2H), 2.40 (d, *J*=6.6, 2H), 2.28 (t, *J*=7.6, 2H), 1.88 – 1.38 (m, 10H), 1.21 (s, 24H), 0.82 (t, *J*=6.2, 3H). ¹³C NMR (300 MHz, MeOD) δ = 184.14, 182.29, 175.55, 40.18, 39.29, 37.07, 33.08, 32.87, 32.73, 30.81, 30.68, 30.57, 30.48, 30.37, 27.36, 27.02, 25.65, 24.44, 24.28, 23.74, 14.45. ¹⁹⁵Pt NMR (86 MHz, DMSO-*d*₆): δppm 1233. ESI-MS (positive ion mode): *m/z* [M]⁺: calcd: 812.4297; obsd: 812.4259 Calcd for C₂₈H₆₃Cl₄N₅O₅Pt: C 37.93%, H 7.16%, N 7.90%. Found: C 38.10%, H 7.12%, N 7.92%.

4.4 General Procedure for the Synthesis of Compound **4b1**.

To a solution of **e** (0.38 mmol) in DMF (10 mL) was added a DMF solution (0.5 mL) containing HATU (0.57 mmol). This mixture stirred for 10 min at room temperature. A DMF solution containing **q** (1.5 mmol) and DIPEA (0.92 mmol) was added to the resulting solution. The mixture was stirred at room temperature for 24 h in the dark. The DMF was then removed under vacuum to afford a yellow oil. Compound **4b1** was purified by silica gel column chromatography as a yellow solid with a yield of 47%. ¹H NMR (300 MHz, MeOD) δ = 3.28 – 3.16 (m, 2H), 3.09 (d, *J*=11.2, 11H), 2.63 – 2.42 (m, 2H), 2.35 (d, *J*=7.5, 2H), 2.23 (s, 2H), 1.96 – 1.40 (m, 8H), 1.35 (s, 27H), 1.28 – 0.87 (m, 22H), 0.78 (t, *J*=6.1, 3H). ¹³C NMR (300 MHz, MeOD) δ = 175.19, 174.36, 157.16, 156.55, 81.57, 80.94, 73.18, 46.24, 46.04, 45.81, 37.99, 37.01, 33.02, 32.73, 32.50, 30.76, 30.63, 30.51, 30.43, 30.29, 30.19, 28.83, 26.97, 25.99, 23.69, 19.34, 14.51.

4.5 General Procedure for the Synthesis of Compound **4b**.

Intermediate **4b1** was dissolved in EtOH (10 mL) and stirred at 0 °C for 10 min. Then, 4 M HCl was added dropwise at 0 °C. The reaction mixture stirred at room temperature for 24–48 h and monitored by TLC. The solution typically gave a faint yellow solid as a precipitate. The solid was filtered, washed several times with absolute ethanol, and dried under vacuum to give the pure target compound **4b**. ¹H NMR (300 MHz, MeOD) δ = 3.73 (m, 1H), 3.28 – 2.83 (m, 18H), 2.43 (d, *J*=22.4, 4H), 2.25 – 1.39 (m, 8H), 0.93 (s, 24H), 0.78 (s, 3H). ¹³C NMR (300 MHz, MeOD) δ = 176.16, 170.19, 152.41, 87.01, 73.92, 46.42, 46.24, 34.97, 34.79, 33.13, 33.03, 31.27, 30.71, 30.63, 30.52, 30.43, 30.32, 30.15, 30.03, 26.09, 24.34, 23.69, 19.41, 14.40. ¹⁹⁵Pt NMR (86 MHz, DMSO-*d*₆): δppm 1236. ESI-MS (positive ion mode): *m/z* [M]⁺: calcd: 881.4134; obsd: 881.4167. Calcd for C₃₂H₆₉Cl₅N₆O₅Pt: C 38.81%, H 7.02%, N 8.49%. Found: C 38.89%, H 7.12%, N 8.38%.

4.6 General Procedure for the Synthesis of Compound **4c1**.

To a solution of **e** (0.38 mmol) in DMF (10 mL) was added a DMF solution (0.5 mL) containing HATU (0.57 mmol). This mixture was stirred for 10 min at room temperature. A DMF solution containing **y** (1.5 mmol) and DIPEA (0.92 mmol) was

added to the resulting solution. The mixture was stirred at room temperature for 24 h in the dark. The DMF was then removed under vacuum to afford a yellow oil. Compound **4c1** was purified by silica gel column chromatography as a yellow solid with a yield of 40%. ¹H NMR (300 MHz, CDCl₃) δ = 3.74 (d, *J*=6.1, 2H), 3.22 (s, 16H), 2.60 (d, *J*=32.1, 7H), 1.77 (m, 5H), 1.40 (m, 54H), 0.92 (s, 2H), 0.78 (s, 2H), 0.63 (s, 3H). ¹³C NMR (300 MHz, CDCl₃) δ = 182.08, 173.24, 156.65, 156.21, 155.48, 79.68, 79.42, 79.33, 54.39, 46.85, 45.26, 44.92, 43.95, 42.61, 32.20, 31.96, 31.87, 29.68, 29.63, 29.31, 28.71, 28.45, 27.73, 25.72, 22.64, 18.01, 14.08, 12.35, 8.02.

4.7 General Procedure for the Synthesis of Compound **4c**.

Intermediate **4c1** was dissolved in EtOH (10 mL) and stirred at 0 °C for 10 min. Then, 4 M HCl was added dropwise at 0 °C. The reaction mixture was stirred at room temperature for 24–48 h and monitored by TLC. The solution typically gave a faint yellow solid as a precipitate. The solid was filtered, washed several times with absolute ethanol, and dried under vacuum to give the pure target compound **4c**. ¹H NMR (300 MHz, D₂O) δ = 4.10 – 3.98 (m, 1H), 3.10 (m, 21H), 2.59 (d, *J*=28.9, 4H), 2.42 (s, 3H), 2.24 – 1.58 (m, 12H), 1.31 – 0.97 (m, 6H). ¹³C NMR (300 MHz, D₂O) δ = 179.71, 179.55, 49.15, 48.99, 48.92, 48.75, 40.24, 40.09, 34.46, 34.42, 34.35, 33.74, 30.00, 29.97, 29.90, 27.00, 26.78, 17.62, 7.70. ¹⁹⁵Pt NMR (86 MHz, DMSO-*d*₆): δppm 1234. ESI-MS (positive ion mode): *m/z* [M+Na]⁺: calcd: 893.4276; obsd: 893.4278. Calcd for C₃₂H₇₁Cl₅N₆O₅Pt: C 38.73%, H 7.21%, N 8.47%. Found: C 38.65%, H 7.32%, N 8.42%.

4.8 General Procedure for the Synthesis of Compound **5a1**.

To a solution of **z** (0.38 mmol) in DMF (10 mL) was added a DMF solution (0.5 mL) containing HATU (0.57 mmol). This mixture was stirred for 10 min at room temperature. A DMF solution containing **y** (1.5 mmol) and DIPEA (0.92 mmol) was added to the resulting solution. The mixture stirred at room temperature for 24 h in the dark. The DMF was then removed under vacuum to afford a yellow oil. Compound **5a1** was purified by silica gel column chromatography as a yellow solid in a yield of 39%. ¹H NMR (300 MHz, CDCl₃) δ = 3.05 (dd, *J*=17.1, 18H), 2.49 (d, *J*=8.4, 7H), 1.89 – 1.00 (m, 65H), 0.84 (d, *J*=6.8, 2H), 0.71 (d, *J*=5.7, 2H), 0.55 (s, 3H). ¹³C NMR (300 MHz, CDCl₃) δ = 175.65, 172.54, 165.32, 156.77, 155.60, 79.44, 46.93, 45.38, 44.92, 36.23, 32.01, 31.95, 29.81, 29.76, 29.67, 29.50, 29.44, 29.31, 28.84, 28.56, 27.94, 27.82, 25.85, 25.80, 22.76, 14.19, 8.14.

4.9 General Procedure for the Synthesis of Compound **5a**.

Intermediate **5a1** was dissolved in EtOH (10 mL) and stirred at 0 °C for 10 min. Then, 4 M HCl was added dropwise at 0 °C. The reaction mixture was stirred at room temperature for 24–48 h and monitored by TLC. The solution typically gave a faint yellow solid as a precipitate. The solid was filtered, washed several times with absolute ethanol, and dried under vacuum to give the pure target compound **5a**. ¹H NMR (300 MHz, CDCl₃) δ = 3.02 (m, 13H), 2.33 (m, 5H), 1.38 (s,

32H), 1.19 (s, 11H), 0.74 (m, 4H), 0.52 (m, 2H). ¹³C NMR (300 MHz, CDCl₃) δ = 171.73, 171.42, 155.65, 154.48, 45.81, 44.31, 43.99, 42.65, 35.23, 30.89, 30.83, 28.69, 28.64, 28.55, 28.38, 28.32, 28.19, 27.72, 27.44, 26.75, 24.68, 21.64, 13.07, 7.02. ¹⁹⁵Pt NMR (86 MHz, DMSO-*d*₆): δppm 1611. ESI-MS (positive ion mode): m/z [M+Na]⁺: calcd: 994.5522; obsd: 994.5533. Calcd for C₄₀H₇₉Cl₃N₆O₉Pt: C 44.10%, H 7.31%, N 7.71%. Found: C 44.18%, H 7.29%, N 7.79%.

4.10 General Procedure for the Synthesis of Compound 6a and 7a

The synthetic routes of 6a and 7a have been reported by our group. [14]

4.11 General Procedure for the Synthesis of Compound 8a.

Our group has reported the synthetic route of d. [14] After reaction with succinic anhydride overnight, the intermediate was dissolved in EtOH (10 mL) and stirred at 0 °C for 10 min to give the target compound 8a-1. 8a-1 ¹H NMR (300 MHz, MeOD) δ = 3.17 (s, 3H), 2.98 (m, 9H), 2.61 – 2.32 (m, 4H), 1.85 (m, 10H), 1.55 (d, *J*=6.6, 4H), 1.23 (s, 8H). ¹³C NMR (300 MHz, CDCl₃) δ = 174.85, 172.29, 155.53, 155.39, 81.15, 80.59, 58.04, 50.24, 29.49, 28.68, 28.40, 28.35, 28.25, 28.10. Then, 4 M HCl was added dropwise at 0 °C. The reaction mixture stirred at room temperature for 24–48 h and monitored by TLC. The solution typically gave a faint yellow solid as a precipitate. The solid was filtered, washed several times with absolute ethanol, and dried under vacuum to give the pure target compound 8a. ¹H NMR (300 MHz, MeOD) δ = 3.44 – 3.24 (m, 2H), 3.15 – 2.92 (m, 10H), 1.78 (dt, *J*=44.0, 22.1, 11H). ¹³C NMR (300 MHz, MeOD) δ = 173.01, 171.47, 46.50, 28.29, 28.23, 27.81, 27.75, 27.51.

4.12 In Vitro Cellular Cytotoxicity Assays

Cells seeded in 96-well plates were incubated in a 5% CO₂ atmosphere in 100 μL of complete medium at 37 °C for 24 h. Then, 100 μL of freshly prepared culture medium containing drugs at different concentrations was added and incubated for another 48 h. MTT (5 mg/mL, 20 μL) was added and incubated for 3 h. Finally, the medium was removed, and DMSO (150 μL) was added. The absorbance was measured at 570 nm using a Bio-Rad 680 microplate reader. The IC₅₀ values were calculated using GraphPad Prism software. Technical repetitions and independent experiments were based on three parallel experiments.

For cytotoxicity assays using the PAT inhibitor Spd, a similar procedure as described above was followed, except that A549cisR cells (5000 cells/well) were seeded on a 96-well plate in 100 μL of RPMI and incubated for 24 h at 37 °C. Spd-containing RPMI medium was used for serial dilution of the platinum compound-containing concentrated solutions, and 100 μL/well was added. The cytotoxicity profiles of the compounds were evaluated using the MTT assay.

A PAO, GSH and GSH-Px Preparation Kit (containing reduced and oxidized glutathione) was used for the isolation of PAO, GSH and GSH-Px in A549 and A549cisR cells, and PAO, GSH and GSH-Px concentrations treated with several

agents in the A549 and A549cisR cellular assays were also measured by microplate reader according to the procedure as described in our previous projects. [14]

4.13 In vivo antitumor and antimetastasis assays

In compliance with the Guide for the Care and Use of Laboratory Animals, we chose healthy female BALB/c mice (from the Laboratory Animal Center, Academy of Military Medical Science, Cat. SCXK 2016-0006, Beijing, China) aged 5 weeks, weighing 18–22 g. 4T1 cells (1 × 10⁶ cells per mouse) were injected *via* the tail vein for the determination of lung metastasis and anticancer activity. 4a was dissolved in glucose injection and immediately used after preparation. All animal procedures were performed following the protocol approved by the Institutional Animal Care and Use Committee at Henan University. The projects *in vivo* were approved by the ethical committee with the number of the approved ethical vote HUSOM-2016-316.

For antimetastatic activity *in vivo*, the tumor cells were inoculated for 7 days to ensure the growth of pulmonary metastasis before drug treatment. On day 8, we injected *via* the tail vein compound 4a (5.0 mg/kg, 10 mg/kg, or 20 mg/kg), oxaliplatin (5 mg/kg, positive control), or normal saline (negative control) every two days for a total of four treatments with the randomly grouped mice (n = 8 mice per group). On day 15, we anesthetized and euthanized the mice and removed the lungs. We counted the lung metastasis nodules of each mouse after fixation with 4% paraformaldehyde for 1 day.

For the solid tumor study, tumors were 80–120 mm³ after 1 week. Then, mice were injected *via* the tail vein with 4a (5.0 mg/kg, 10 mg/kg, or 20 mg/kg), oxaliplatin (5 mg/kg, positive control), or physiological saline (negative control) every two days for a total of four treatments. The mice were weighed every two days, and the tumor volume was measured by a Vernier caliper.

The mice were sacrificed by anesthesia and the tumor tissues were removed and weighed. We calculated the inhibition rate as follows: inhibition rate (%) = [(average tumor weight of negative control group – average tumor weight of the drug treated or positive control group)/average tumor weight of control group] × 100. Moreover, on the last day, we removed and weighed the organs (heart, liver, kidney, lung, and spleen) of the mice. We calculated the organ weight index as follows: organ index (%) = (organ weight/body weight) × 100%

4.14 In vivo MTD and LD₅₀ antitumor assays

The maximum tolerated dose (MTD) (n = 10 mice per group) was evaluated by calculating body weight loss (mean weight loss <15% and <15% toxic deaths) and the lethal dose values (LD₅₀) (n = 10 mice per group) were determined. The TI value was calculated according to the procedure as previous described. [12b]

4.15 Transwell Migration Assay

Transwell migration assays were performed by using modified Boyden's chamber in 24-well cell culture plate with a 8 μm pore. Chambers were washed with PBS for three times. Then

the medium with the tested compound was placed in the lower chamber, and cells were seeded in the top chamber. Cells were treated with **4a** or cisplatin at 37 °C in a humidified atmosphere of 5% CO₂. After incubation for 24 h, non-migrated cells on the top surface of the membrane were gently scraped away with cotton swab. The migrated-cells was fixed with 4% paraformaldehyde for 20 min and stained with 0.2% crystal violet. Images were recorded using a Leika inverted microscope.

4.16 Cellular Platinum Uptake and DNA Platination

Cellular uptake was measured in A549, A549cisR, SMMC-7721, and MCF-7 cells. A549, A549cisR, SMMC-7721, and MCF-7 cells were seeded in 6-well plates overnight and then incubated with 10 μM homospermidineplatin **4a** or cisplatin for 8 h. Subsequently, the cells were washed with PBS buffer three times and harvested by trypsinization. The harvested cells were concentrated and digested with nitric acid for ICP-MS. The cell numbers were counted before digestion. A Genomic DNA mini preparation kit was used for the isolation of DNA in A549, A549cisR, SMMC-7721, and MCF-7 cells, and Pt concentrations in the cellular DNA of A549, A549cisR, SMMC-7721, and MCF-7 cells digested by nitric acid were also measured by ICP-MS.

4.17 Annexin V-FITC/Propidium Iodide Staining

Apoptosis of A549cisR cells was evaluated using Annexin V-FITC/PI staining detected by flow cytometry. Cells were plated into six-well plates at 1×10^5 cells/well. After cultured for 24 h, cells were hatched with **4a** (5 or 10 μM), cisplatin (15 μM) for 24 h. Then cells were harvested, washed three times with PBS to remove unbound dyes, and stained according to the manufacturer's protocol. Analysis was performed by flow cytometry (BD Biosciences, San Jose, CA, USA).

4.18 Western Blot Assay

To detect the expression of the related proteins phospho-histone H2A-X (Ser139), p53, ODC and SSAT, Western blot analysis was performed. Cells were treated with **4a** at concentrations of 5, 10, and 15 μM for 24 h and were then harvested and centrifuged. The cell pellets were washed three times with ice-cold PBS and then lysed with RIPA buffer (Beyotime, China). Using a BCA assay kit (Beyotime, China), we determined the total concentration of protein. After that, we denatured the total lysates in 5 × SDS-loading buffer at 100 °C for 10 min. Using 12% SDS-PAGE for 2 h, we separated equal amounts of total proteins and then transferred the proteins onto PVDF membranes. The membranes were blocked with 5% dried skimmed milk in TBST at room temperature for 1 h. After incubation with the corresponding primary antibodies overnight at 4 °C, the membranes were washed three times with TBST and incubated with the appropriate HRP-conjugated secondary antibody. Protein expression was detected using the ECL plus reagents (Beyotime, Jiangsu, China).

4.19 Detection of polyamine oxidase (PAO)

Total PAO level was measured using GSH assay kit according to the manufacturer's instructions ((Hepeng Biotechnology, Cat. HEPENGBIO156). Briefly, after treatment with **4a** (10 μM) for 24 h, cells were washed twice with Reagent A (3 mL) and then collected the cells by cell scraper. Pellets were resuspended in Reagent A (3 mL) by centrifugation at 300g for 5 min. Supernate were resuspended in Reagent B (500 μL) and vortexed immediately followed by being lysed by three freeze-thaw cycles. After cell lysates were centrifuged at 16,000g for 5 min at 4 °C, supernatant containing total PAO was transferred to another pre-cooling tube. For quantifying total PAO level, 10 μL of supernatant was mixed with 240 μL (200 μL Reagent C, 25 μL Reagent D and 15μL Reagent E) of total PAO assay buffer for 3 min at 37 °C, and then 10 μL of Reagent F was added. Absorbance was read at 440 nm by using the microplate reader.

4.20 Reactive Oxygen Species Assay

Reactive oxygen species (ROS) were examined with the fluorescent probe DCFH-DA and detected by flow cytometry as our previously described . [14]

4.21 Detection of total glutathione (GSH)

Total glutathione (containing reduced and oxidized glutathione) level was measured using GSH assay kit according to the manufacturer's instructions (Solarbio Biochemical Assay Division, Cat. 20180226, Beijing, China). Briefly, after treatment with **4a** (10 μM) for 24 h, cells were washed twice with PBS by centrifugation at 600g for 5 min. Pellets were resuspended in protein removal buffer and vortexed immediately followed by being lysed by three freeze-thaw cycles. After cell lysates were centrifuged at 12,000g for 10 min at 4 °C, supernatant containing total glutathione was transferred to another tube. For quantifying total glutathione level, 10 μL of supernatant was mixed with 150 μL of total glutathione assay buffer for 5 min, and then 50 μL of NADPH (0.16 mg/mL) was added. Absorbance was read at 405 nm by using the microplate reader.

4.22 Detection of total glutathione peroxidase (GSH-Px)

Total GSH-Px level was measured using GSH-Px assay kit according to the manufacturer's instructions (Leagene Biotechnology, Cat. 0309A18, Beijing, China). Briefly, after treatment with **4a** (10 μM) for 24 h, cells were washed twice with PBS by centrifugation at 12, 000g for 10 min. Pellets were resuspended in protein removal buffer and vortexed immediately followed by being lysed by three freeze-thaw cycles. After cell lysates were centrifuged at 12,000g for 10 min at 4 °C, supernatant containing total GSH-Px was transferred to another tube. For quantifying total GSH-Px level, 0.2 mL of supernatant was mixed with 0.4 mL of total GSH-Px assay buffer for 5 min at 37 °C, and then 0.25 mL of benzoic acid was added. Absorbance was read at 422 nm by using the microplate reader.

4.23 Polyamines Contents Assay

Coupled with a G1321A fluorescence detector, we quantified the polyamine (putrescine, spermidine, and spermine) content in A549cisR cells by using HPLC (Agilent 1260, Agilent Technologies, USA) according to our previous reported. [14]

The polyamines were separated on a C18 chromatographic column (25 × 4.6 mm, 5 μm) with dansyl chloride as the derivatization reagent and 1,6-diaminohexane as the internal standard substance using methanol–water (65:35–100:0, 30 min gradient elution) (excitation = 340 nm and emission = 515 nm). The polyamines (putrescine, spermidine, and spermine) were converted to the corresponding dansyl derivatives and separated on a C18 analytical column by eluting with an ethyl acetate/water gradient. 1,6-Diaminohexane was used as the internal standard.

ASSOCIATED CONTENT

The Supporting Information is available free of charge on the ACS Publications website.

Full experimental details, NMR data, and bioassay information (PDF)

Molecular formula strings(CSV)

AUTHOR INFORMATION

Corresponding Author *Phone: (86) 0371-23880680. Fax: (86) 0371-23880680. E-mail: majing@henu.edu.cn; wjcsxq@henu.edu.cn; xiesq@vip.henu.edu.cn

Author Contributions

#The authors contribute equally to this work.

Abbreviations

PTs, Polyamine Transporters; SSAT, spermidine/spermine N1-acetyltransferase; PAO, N1-acetylpolyamine oxidase; ROS, Reactive Oxygen Species; GSH-Px, glutathione peroxidase; GSH, glutathione; Spd, spermidine; Spm, spermine; Put, putrescine. LD₅₀, lethal dose of 50%; MTD, maximum tolerated dose; IC₅₀, half maximal inhibitory concentration; ICP-MS, Inductively Coupled Plasma Mass Spectrometry; DMF, dimethyl formamide; DIPEA, diisopropylethylamine; HATU, 2-(7-Azabenzotriazol-1-yl)-N,N,N',N'-tetramethyluronium hexafluorophosphate.

Notes

The authors declare no competing financial interest.

ACKNOWLEDGMENTS

This work was supported by National Natural Science Foundation of China (Grant No. 21807025, 81772832 and 81573465), China Postdoctoral Science Foundation (Grant No. 2018M640673), Postdoctoral Research Grant in Henan Province (Grant No. 001802020), Key Scientific Research Projects in Henan Colleges and Universities (Grant No. 19A350002), Program for Innovative Research Team (in

Science and Technology in University of Henan Province) (Grant No. 19IRTSTHN004), Project of Innovation and Entrepreneurship Support Program for College Students of Henan University Minsheng College (Grant No. MSCXCY2018058) and Henan University (Grant No. 201910475012 and 2019102004), Scientific Research Cultivating Program for Young Talents in Henan Medical School (Grant No. 2019006) and the key scientific research projects of universities in Henan province (No13A350095).

REFERENCES

- [1] Forner, A.; Llovet, J. M.; Bruix, Hepatocellular carcinoma. *J. Lancet* 2012, 379, 1245–1255.
- [2] Dou, C.; Liu, Z.; Xu, M.; Jia, Y.; Wang, Y.; Li, Q.; Yang, W.; Zheng, X.; Tu, K.; Liu, Q. miR-187-3p inhibits the metastasis and epithelial-mesenchymal transition of hepatocellular carcinoma by targeting S100A4. *Cancer Lett.* 2016, 381, 380–390
- [3] Valastyan, S.; Weinberg, R. A. Tumor metastasis: molecular insights and evolving paradigms. *Cell* 2011, 147, 275–292.
- [4] Sonnenschein, C.; Soto, A. M. Cancer metastases: so close and so far. *J. Natl. Cancer Inst.* 2015, 107, djv236.
- [5] Ran, S. The role of TLR4 in chemotherapy-driven metastasis. *Cancer Res.* 2015, 75, 2405–2410.
- [6] Johnstone, T.C.; Suntharalingam, K.; Lippard, S.J. The Next generation of platinum drugs: targeted Pt(II) agents, nanoparticle delivery, and Pt(IV) prodrugs. *Chem Rev.* 2016, 116, 3436–3486.
- [7] a) Kenny RG, Marmion CJ. Toward multi-targeted platinum and ruthenium drugs-a new paradigm in cancer drug treatment regimens? *Chem Rev.* 2019, 119, 1058–1137; b) Wang, D.; Lippard, S. J. Cellular processing of platinum anticancer drugs. *Nat. Rev. Drug Discovery* 2005, 4, 307 – 320; c) Wheate, N. J.; Walker, S.; Craig, G. E.; Oun, R. The status of platinum anticancer drugs in the clinic and in clinical trials. *Dalton Trans.* 2010, 39, 8113–8127. d) L. Kelland, The resurgence of platinum-based cancer chemotherapy. *Nat. Rev. Cancer* 2007, 7, 573–584.
- [8] Wang, X.; Wang, X.; Guo, Z. Functionalization of platinum complexes for biomedical applications. *Acc Chem Res.* 2015, 48, 2622–2631.
- [9] Basu, U.; Banik, B.; Wen, R.; Pathak, R.K.; Dhar, S. The platin-X series: activation, targeting, and delivery. *Dalton Trans.* 2016, 45, 12992–3004.
- [10] Han, X.; Sun, J.; Wang, Y.; He, Z. Recent advances in platinum (IV) complex-based delivery systems to improve platinum (II) anticancer therapy. *Med Res Rev.* 2015, 35, 1268–1299.
- [11] a) Chen, Y.; Heeg, M. J.; Braunschweiger, P. G.; Xie, W.; Wang, P. G. A carbohydrate-linked cisplatin analogue having antitumor activity. *Angew. Chem., Int. Ed.* 1999, 38: 1768; b) Ma, J.; Wang, Q.; Yang, X.; Hao, W.; Huang, Z.; Zhang, J.; Wang, X.; Wang, P. Glycosylated platinum(IV) prodrugs demonstrated significant therapeutic efficacy in cancer cells and minimized side-effects. *Dalton Trans.* 2016, 45: 11830–11838. c) Wang, Q.; Huang, Z.; Ma, J.; Lu, X.; Zhang, L.; Wang, X.; Wang, P. G. Design, synthesis and biological evaluation of a novel series of glycosylated platinum(IV) complexes as antitumor agents. *Dalton Trans.* 2016, 45:

- 10366–10374. d) Ma, J.; Wang, Q.; Huang, Z.; Yang, X.; Nie, Q.; Hao, W.; Wang, P.G.; Wang, X. Glycosylated platinum(IV) complexes as substrates for glucose transporters (GLUTs) and organic cation transporters (OCTs) exhibited cancer targeting and human serum albumin binding properties for drug delivery. **J Med Chem.** 2017, 60: 5736-5748. e) Ma, J.; Yang, X.; Hao, W.; Huang, Z.; Wang, X.; Wang, P.G. Mono-functionalized glycosylated platinum(IV) complexes possessed both pH and redox dual-responsive properties: exhibited enhanced safety and preferentially accumulated in cancer cells in vitro and in vivo. **Eur J Med Chem.** 2017, 128: 45-55. f) Ma J, Liu H, Xi Z, Hou J, Li Y, Niu J, Liu T, Bi S, Wang X, Wang C, Wang J, Xie S, Wang PG. Protected and de-protected platinum(IV) glycoconjugates with GLUT1 and OCT2-mediated selective cancer targeting: demonstrated enhanced transporter-mediated cytotoxic properties in vitro and in vivo. **Front Chem.** 2018, 6, 386. g) Wang H, Yang X, Zhao C, Wang PG, Wang X. Glucose-conjugated platinum(IV) complexes as tumor-targeting agents: design, synthesis and biological evaluation. **Bioorg Med Chem.** 2019, 27, 1639-1645.
- [12] a). Dhar S, Daniel WL, Giljohann DA, Mirkin CA, Lippard SJ. Polyvalent oligonucleotide gold nanoparticle conjugates as delivery vehicles for platinum(IV) warheads. **J Am Chem Soc.** 2009, 131, 14652-14653. b). Liu P, Lu Y, Gao X, Liu R, Zhang-Negrerie D, Shi Y, Wang Y, Wang S, Gao Q. Highly water-soluble platinum(II) complexes as GLUT substrates for targeted therapy: improved anticancer efficacy and transporter-mediated cytotoxic properties. **Chem Commun.** 2013, 49, 2421-2423. c). Y.-R. Zheng, K. Suntharalingam, T. C. Johnstone, H. Yoo, W. Lin, J. G. Brooks, S. J. Lippard, Pt(IV) prodrugs designed to bind non-covalently to human serum albumin for drug delivery. **J. Am. Chem. Soc.** 2014, 136, 8790-8798; d). Q. Cheng, H. Shi, H. Wang, Y. Min, J. Wang, Y. Liu, The ligation of aspirin to cisplatin demonstrates significant synergistic effects on tumor cells. **Chem. Commun.** 2014, 50, 7427-7430; e). R. K. Pathak, S. Marrache, J. H. Choi, T. B. Berding, S. Dhar, The prodrug platin-A: simultaneous release of cisplatin and aspirin. **Angew. Chem. Int. Ed.** 2014, 53, 1963-1967; f). S. G. Awuah, Y. R. Zheng, P. M. Bruno, M. T. Hemann, S. J. Lippard, A Pt(IV) pro-drug preferentially targets indoleamine-2,3-dioxygenase, providing enhanced ovarian cancer immuno-chemotherapy. **J. Am. Chem. Soc.** 2015, 137, 14854-14857; g). J. Kasparkova, H. Kostrhunova, O. Novakova, R. Kr'ikavov J. Vanc'ok, V. Brabec, A photoactivatable platinum(IV) complex targeting genomic DNA and histone deacetylases. **Angew. Chem. Int. Ed.** 2015, 54, 14478-14482; h). R. Raveendran, J. P. Braude, E. Wexselblatt, V. Novohradsky, O. Stuchlikova, V. Brabec, V. Gandin, D. Gibson, Pt(iv) derivatives of cisplatin and oxaliplatin with phenylbutyrate axial ligands are potent cytotoxic agents that act by several mechanisms of action. **Chem. Sci.** 2016, 7, 2381-2391; i). G. Thiabaud, R. McCall, G. He, J. F. Arambula, Z. H. Siddik, J. L. Sessler, Activation of platinum(IV) prodrugs by motexafin gadolinium as a redox mediator. **Angew. Chem. Int. Ed.** 2016, 55, 12626-12631; j). N. Muhammad, N. Sadia, C. Zhu, C. Luo, Z. Guo, X. Wang, Biotin-tagged platinum(iv) complexes as targeted cytostatic agents against breast cancer cells. **Chem. Commun.** 2017, 53, 9971 – 9974; k). E. Petruzzella, J. P. Braude, J. R. AldrichWright, V. Gandin, D. Gibson, A quadruple-action platinum(IV) prodrug with anticancer activity against KRAS mutated cancer cell lines. **Angew. Chem. Int. Ed.** 2017, 56, 11539 – 11544; l). Ma L, Wang N, Ma R, Li C, Xu Z, Tse MK, Zhu G. Monochalcoplatin: an actively transported, quickly reducible, and highly potent Pt(IV) anticancer prodrug. **Angew. Chem. Int. Ed.** 2018, 57, 9098-9102. m). Petruzzella E, Sirota R, Solazzo I, Gandin V, Gibson D. Triple action Pt(iv) derivatives of cisplatin: a new class of potent anticancer agents that overcome resistance. **Chem Sci.** 2018, 9, 4299-4307. n). Wang K, Zhu C, He Y, Zhang Z, Zhou W, Muhammad N, Guo Y, Wang X, Guo Z. Restraining cancer cells by dual metabolic inhibition with a mitochondrion-targeted platinum(II) complex. **Angew. Chem. Int. Ed.** 2019, 58, 4638-4643; o). Zhu Z, Wang Z, Zhang C, Wang Y, Zhang H, Gan Z, Guo Z, Wang X. Mitochondrion-targeted platinum complexes suppressing lung cancer through multiple pathways involving energy metabolism. **Chem Sci.** 2019, 10, 3089-3095; p). Babak MV, Zhi Y, Czarny B, Toh TB, Hooi L, Chow EK, Ang WH, Gibson D, Pastorin G. Dual-targeting dual-action platinum(IV) platform for enhanced anticancer activity and reduced nephrotoxicity. **Angew. Chem. Int. Ed.** 2019, 58, 8109-8114. q). Chen F, Huang X, Wu M, Gou S, Hu W. A CK2-targeted Pt(IV) prodrug to disrupt DNA damage response. **Cancer Lett.** 2017, 385, 168-178. r). Chun W, Ke-Jia W, Jin-Biao L, Xiao-Ming Z, Chung-Hang L and Dik-Lung M. A dual-functional molecular strategy for in situ suppressing and visualizing of neuraminidase in aqueous solution using iridium(iii) complexes. **Chem. Commun.**, 2019, 55, 6353. s). Guan-Jun Y, Wanhe W, Simon Wing FM, Chun W, Betty Yuen KL, Xiang-Min M, Ke-Jia W, Hai-Jing Z, Chun-Yuen W, Vincent Kam W, DikLung M and Chung-Hang L. Selective inhibition of lysine-specific demethylase 5A (KDM5A) using a rhodium(III) complex for triple-negative breast cancer therapy. **Angew. Chem. Int. Ed.** 2018, 57, 13091. t). Huaiyi H, Samya B, Kangqiang Q, Pingyu Z, Olivier B, Thomas M, Martin J. P, Guy J. C, Michael S, Vasilios G. S, Gilles G, Hui C and Peter J. S. Targeted photoredox catalysis in cancer cells. **Nat. Chem.**, 2019, DOI: 10.1038/s41557-019-0328-4.
- [13] a). Casero RA Jr, Murray Stewart T, Pegg AE. Polyamine metabolism and cancer: treatments, challenges and opportunities. **Nat Rev Cancer.** 2018, 18, 681-695. b). Phanstiel O 4th. An overview of polyamine metabolism in pancreatic ductal adenocarcinoma. **Int J Cancer.** 2018, 142, 1968-1976. c). Casero RA Jr, Marton LJ. Targeting polyamine metabolism and function in cancer and other hyperproliferative diseases. **Nat Rev Drug Discov.** 2007, 6, 373-90. d). Muth, A.; Pandey, V.; Kaur, N.; Wason, M.; Baker, C.; Han, X.; Johnson, T. R.; Altomare, D. A.; Phanstiel, O., 4th Synthesis and biological evaluation of antimetastatic agents predicated upon dihydromotuporamine C and its carbocyclic derivatives. **J. Med. Chem.** 2014, 57, 4023–4034. e). Skruber, K.; Chaplin, K. J.; Phanstiel, O., 4th. Synthesis and bioevaluation of macrocycle-polyamine conjugates as cell migration inhibitors. **J. Med. Chem.** 2017, 60, 8606–8619. f). Muth A, Kamel J, Kaur N, Shicora AC, Ayene IS, Gilmour SK, Phanstiel O 4th. Development of polyamine transport ligands with improved metabolic stability and selectivity against specific human cancers. **J Med Chem.** 2013, 56, 5819-5828.
- [14] a). Chaojie, W.; Jean-Guy, D.; Laura, C.; Fanta, K.; Horacio, C.; John, B.; Richard Andrew, G.; Phanstiel O 4th.

- Defining the molecular requirements for the selective delivery of polyamine conjugates into cells containing active polyamine transporters. **J Med Chem.** 2003, 46, 5129-5138.
- b). Chaojie, W.; Jean-Guy, D.; John, B.; Phanstiel O 4th. Molecular requirements for targeting the polyamine transport system. Synthesis and biological evaluation of polyamine-anthracene conjugates. **J Med Chem.** 2003, 46, 2672-2682.
- c). Chaojie, W.; Jean-Guy, D.; John, B.; Phanstiel O 4th. Synthesis and biological evaluation of N1-(anthracen-9-ylmethyl)triamines as molecular recognition elements for the polyamine transporter. **J Med Chem.** 2003, 46, 2663-2671.
- d). Xie, S.; Wang, J.; Zhang, Y.; Wang, C. Antitumor conjugates with polyamine vectors and their molecular mechanisms. **Expert Opin Drug Deliv.** 2010, 7, 1049-1061.
- e). Wang, Y. X.; Zhang, X.; Zhao, J.; Xie, S. Q.; Wang, C. J. Nonhematotoxic naphthalene diimide modified by polyamine: synthesis and biological evaluation. **J. Med. Chem.** 2012, 55, 3502-3512.
- f). Li, M.; Li, Q.; Zhang, Y. H.; Tian, Z. Y.; Ma, H. X.; Zhao, J.; Xie, S. Q.; Wang, C. Antitumor effects and preliminary systemic toxicity of ANISpm in vivo and in vitro. **Anti-Cancer Drugs** 2013, 24, 32-42.
- g). Li, Q.; Zhai, Y.; Luo, W.; Zhu, Z.; Zhang, X.; Xie, S.; Hong, C.; Wang, Y.; Su, Y.; Zhao, J.; Wang, C. Synthesis and biological properties of polyamine modified flavonoids as hepatocellular carcinoma inhibitors. **Eur. J. Med. Chem.** 2016, 121, 110-119.
- h). Dai, F. J.; Li, Q.; Wang, Y. X.; Ge, C. C.; Feng, C.; Xie, S. Q.; He, H.; Xu, X.; Wang, C. J. Design, synthesis, and biological evaluation of mitochondria-targeted flavone-naphthalimide-polyamine conjugates with antimetastatic activity. **J. Med. Chem.** 2017, 60, 2071-2083.
- i). Li J, Tian R, Ge C, Chen Y, Liu X, Wang Y, Yang Y, Luo W, Dai F, Wang S, Chen S, Xie S, Wang C. Discovery of the polyamine conjugate with benzo[cd]indol-2(1H)-one as a lysosome-targeted antimetastatic agent. **J Med Chem.** 2018, 61, 6814-6829.
- j). Cong W, Ping R, Ying Z, Xiaomin L, Jun W, Xiaoxiao W, Tong L, Shasha W, Jiuzhou H, Wei L, Qian L, Jinghua L, Fujun D, Dong F, Chaojie W, Songqiang X. Spermidine/spermine N1-acetyltransferase regulates cell growth and metastasis via AKT/ β -catenin signaling pathways in hepatocellular and colorectal carcinoma cells. **Oncotarget**, 2017, 8, 1092-1109.
- [15] a) Li L, Mao Y, Zhao L, Li L, Wu J, Zhao M, Du W, Yu L, Jiang P. p53 regulation of ammonia metabolism through urea cycle controls polyamine biosynthesis. **Nature.** 2019, 567, 253-256. b) Ou Y, Wang SJ, Li D, Chu B, Gu W. Activation of SAT1 engages polyamine metabolism with p53-mediated ferroptotic responses. **Proc Natl Acad Sci U S A.** 2016, 113, E6806-E6812. c). Eastman A. Improving anticancer drug development begins with cell culture: misinformation perpetrated by the misuse of cytotoxicity assays. **Oncotarget.** 2017, 8, 8854-8866. d). Mirzayans R, Andrais B, Murray D. Do Multiwell Plate High Throughput Assays Measure Loss of Cell Viability Following Exposure to Genotoxic Agents? **Int J Mol Sci.** 2017, 18, 1679.
- [16] Nguyen, D. X.; Bos, P. D.; Massague, J. Metastasis: from dissemination to organ-specific colonization. **Nat. Rev. Cancer** 2009, 9, 274-284.
- [17] W. M. Bonner, C. E. Redon, J. S. Dickey, A. J. Nakamura, O. A. Sedelnikova, S. Solier, Y. Pommier, GammaH2AX and cancer. **Nat. Rev. Cancer** 2008, 8, 957-967.
- [18] Ishikawa T. The ATP-dependent glutathione S-conjugate export pump. **Trends Biochem Sci.** 1992, 11, 463-468.
- [19] Yang, L.; Zhao, J.; Zhu, Y.; Tian, Z.; Wang, C. Reactive oxygen species (ROS) accumulation induced by mononaphthalimide-spermidine leads to intrinsic and AIF-mediated apoptosis in HeLa cells. **Oncol. Rep.** 2011, 25 (4), 1099-1107.

1
2
3
4
5
6
7
8
9
10
11
12
13
14
15
16
17
18
19
20
21
22
23
24
25
26
27
28
29
30
31
32
33
34
35
36
37
38
39
40
41
42
43
44
45
46
47
48
49
50
51
52
53
54
55
56
57
58
59
60

Table of Contents Graphic

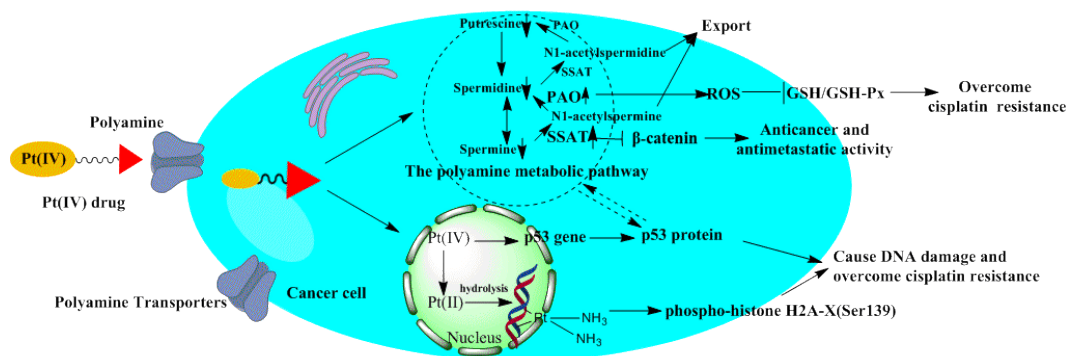


Table of Contents Graphic

